UTPT-97-1

THE LIGHT–FRONT MODEL FOR EXCLUSIVE SEMILEPTONIC B– AND D–DECAYS

N. B. Demchuk, P. Yu. Kulikov, I. M. Narodetskii
Institute of Theoretical and Experimental Physics,
117259 Moscow, RF
and
Patrick J. O'Donnell,
Physics Department, University of Toronto,
Ontario M5S 1A7, Canada

arXiv:hep-ph/9701388v2 12 Feb 1997

Abstract

An explicit relativistic light-front quark model is presented which gives the momentum transfer dependent form factors of weak hadronic currents among heavy pseudoscalar and vector mesons in the whole accessible kinematic region $0 \leq q^2 \leq q^2_{max}$. For the numerical investigations of the $B \to D^* l\nu_l$, $B \to \rho l\nu_l$, $D \to K^* l\nu_l$ and $D \to \rho l\nu_l$ semileptonic decays the equal time wave functions corresponding to the updated version of the ISGW model are adopted. Using the available experimental information on branching fractions $BR(B \to D^* l\nu_l)$ and $BR(B \to \rho l\nu_l)$ the CKM parameters V_{cb} and V_{ub} were estimated: $|V_{cb}| = 0.036 \pm 0.004$, $|V_{ub}| = 0.0033 \pm 0.0004$. The model is further tested by comparison with experimental data, QCD sum rules and lattice calculations.

PACS numbers: 13.20 He; 13.20 Fc; 12.39 Ki; 12.15 Hh
Keywords: semileptonic decays; heavy mesons, relativistic quark models

1 Introduction

The knowledge and understanding of the form factors of hadronic currents is of decisive importance for the determination of the quark mixing parameters. In heavy–to–heavy transitions the determination of these form factors can be obtained based on heavy-quark symmetry in a nearly model–independent way [1]. On the other hand, in the theoretical description of the heavy–to–light decays there is no symmetry one can apply to constrain the relevant hadronic form factors. Quark model (QM) calculations can be very helpful for heavy–to–heavy as well as for heavy–to–light transitions [2]. Although strict theoretical error limits cannot be given, they provide a vivid picture of what is going on and give numerous testable predictions for quite different processes.

In refs. [3, 4] the q^2 dependence of the form factors among various pseudoscalar mesons has been calculated in the whole accessible kinematic region $0 \leq q^2 \leq q^2_{max}$ using the light-front (LF) QM. The calculations have been performed in a reference frame where the momentum transfer is purely longitudinal. The form factors were determined by using matrix elements of the plus components of the currents which are "good" operators in the LF formalism [5]. The purpose of this paper is to generalize the results of refs. [3, 4] and extend them for the calculations of the form factors governing pseudoscalar–vector $(PS-V)$ transitions to 1^- states. We will show that the latter can again be expressed in terms of the matrix elements of the plus components of the currents in a reference frame corresponding to the purely longitudinal momentum transfers, but the calculations require the use of a limiting procedure.

The plan of the paper is as follows. In Sections 2–4 we describe our approach for the calculation of the weak meson form factors. In Section 5 the numerical results for the form factors and the exclusive decay rates of the $B \to D(D^*)\ell\nu_\ell$, $B \to \pi(\rho)\ell\nu_\ell$, $D \to K(K^*)\ell\nu_\ell$ and $D \to \pi(\rho)\ell\nu_\ell$ weak decays are presented and compared with experimental data as well as with the results of other approaches. Section 6 contains a brief summary.

2 Kinematics

We denote by P_1, P_2 and M_1, M_2 the 4-momentum and masses of the parent and daughter mesons, respectively. The meson states are denoted as $|P>$ for a pseudoscalar state and $|P,\varepsilon>$ for a vector state, where ε is the polarization vector, satisfying $\varepsilon \cdot P = 0$. The 4-momentum transfer q is given by $q = P_1 - P_2$ and the momentum fraction r is defined as

$$r = \frac{P_2^+}{P_1^+} = 1 - \frac{q^+}{P_1^+}. \tag{1}$$

In the following we work in the rest frame of the parent meson. The 3-momentum $\mathbf{P_2}$ of the final meson is in the plane 1-3, so that $\mathbf{q}_\perp \neq 0$. We denote the angle between $\mathbf{P_2}$ and the 3-axis by α. Then, it can be easily verified that

$$q^2 = (1-r)(M_1^2 - \frac{M_2^2}{r}) - \frac{q_\perp^2}{r}, \tag{2}$$

$$q_\perp^2 = M_2^2(y^2-1)\sin^2\alpha, \tag{3}$$

where the"velocity transfer" y is defined as $y = u_1 \cdot u_2$ with u_1 and u_2 being the 4-velocities of the initial and final mesons. The relation between y and q^2 is given by

$$y = \frac{M_1^2 + M_2^2 - q^2}{2M_1 M_2}. \tag{4}$$

The momentum fraction of Eq. (1) is invariant under the boosts along the 3− axis and the rotations around this axis but depends explicitly on the recoil direction. Solving Eq. (2) for r one obtains

$$r(q^2, \alpha) = \zeta(y + \sqrt{y^2 - 1}\cos\alpha), \tag{5}$$

where $\zeta = \frac{M_2}{M_1}$. At the point of zero recoil r does not depend on α, $r(q^2_{max}) = \zeta$.

The hadronic form factors for semileptonic decays are defined as the Lorentz–invariant functions arising in the covariant decomposition of matrix elements of the vector and axial currents. We define the form factors of the $P_1(Q_1\bar{q}) \to P_2(Q_2\bar{q})$ transitions between the ground state S–wave mesons in the usual way. The amplitude $< P_2|V_\mu|P_1 >=< P_2|\bar{Q}_2\gamma_\mu Q_1|P_1 >$ can be expressed in terms of two form factors

$$< P_2|V_\mu|P_1 >= \left(P_\mu - \frac{M_1^2 - M_2^2}{q^2}q_\mu\right) F_1(q^2) + \frac{M_1^2 - M_2^2}{q^2}q_\mu F_0(q^2), \tag{6}$$

where $P = P_1 + P_2$. There is one form factor for the amplitude $< P_2, \varepsilon|V_\mu|P_1 >$

$$< P_2, \varepsilon|V_\mu|P_1 >= \frac{2i}{M_1 + M_2}\varepsilon_{\mu\nu\alpha\beta}\varepsilon^{*\nu}P_1^\alpha P_2^\beta V(q^2), \tag{7}$$

and three independent form factors for the amplitude $< P_2, \varepsilon|A_\mu|P_1 >=< P_2, \varepsilon|\bar{Q}_2\gamma_\mu\gamma_5 Q_1|P_1 >$

$$\begin{aligned} < P_2, \varepsilon|A_\mu|P_1 > \;\; = \;\; & \left((M_1 + M_2)\varepsilon^{*\mu}A_1(q^2) - \frac{\varepsilon^* q}{M_1 + M_2}(P_1 + P_2)_\mu A_2(q^2) - 2M_2\frac{\varepsilon^* q}{q^2}q_\mu A_3(q^2)\right) \\ & +2M_2\frac{\varepsilon^* q}{q^2}q_\mu A_0(q^2), \end{aligned} \tag{8}$$

where $A_0(0) = A_3(0)$ and the form factor $A_3(q^2)$ is given by the linear combination

$$A_3(q^2) = \frac{M_1 + M_2}{2M_2}A_1(q^2) - \frac{M_1 - M_2}{2M_2}A_2(q^2). \tag{9}$$

Sometimes another set of form factors is introduced

$$< P_2, \varepsilon|V_\mu|P_1 >= ig(q^2)\varepsilon_{\mu\nu\alpha\beta}\varepsilon^{*\nu}P^\alpha q^\beta, \tag{10}$$

$$< P_2, \varepsilon|A_\mu|P_1 >= -\left[f(q^2)\varepsilon^*_\mu + a_+(q^2)(\varepsilon^* P)P_\mu + a_-(q^2)(\varepsilon^* P)q_\mu\right]. \tag{11}$$

The relationship between two sets of form factors is given by

$$V(q^2) = -(M_1 + M_2)g(q^2), \tag{12}$$

$$A_0(q^2) = -\frac{1}{2M_2}[f(q^2) + (M_1^2 - M_2^2)a_+(q^2) + q^2 a_-(q^2)], \tag{13}$$

$$A_1(q^2) = -\frac{f(q^2)}{M_1 + M_2}, \tag{14}$$

$$A_2(q^2) = (M_1 + M_2)a_+(q^2). \tag{15}$$

In the massless lepton limit the form factors $F_0(q^2)$ and $a_-(q^2)$ do not contribute to the decay rates because of leptonic current conservation. The differential decay width for a semileptonic decay of a PS particle to another PS particle and a massless lepton pair ($e\bar{\nu}_e$ or $\mu\bar{\nu}_\mu$) is given by

$$\frac{d\Gamma}{dy} = \frac{G_F^2 M_1^5}{12\pi^3}\zeta^4 |V_{Q_1Q_2}|^2 (y^2-1)^{3/2} |F_1(y)|^2, \tag{16}$$

where $V_{Q_1Q_2}$ is the CKM matrix element. The differential transition rate to a vector particle is

$$\frac{d\Gamma}{dy} = \frac{G_F^2 M_1}{48\pi^3}\zeta^2 |V_{Q_1Q_2}|^2 (y^2-1)^{1/2} q^2 (H_+^2 + H_-^2 + H_0^2), \tag{17}$$

where the helicity amplitudes are given by

$$H_0 = \frac{M_1^2}{\sqrt{q^2}}\left((y-\zeta)(1+\zeta)A_1(y) - 2(y^2-1)\zeta\frac{A_2(y)}{1+\zeta}\right), \tag{18}$$

$$H_\pm = M_1\left((1+\zeta)A_1(y) \mp 2(y^2-1)^{1/2}\zeta\frac{V(y)}{1+\zeta}\right). \tag{19}$$

Near the kinematic point of zero recoil, $y = 1$, Eq. (17) simplifies to [6]

$$\frac{d\Gamma}{dy} = \frac{G_F^2 M_1^5}{16\pi^3}\zeta^2 |V_{Q_1Q_2}|^2 (1-\zeta)^2 (y^2-1)^{1/2} |A_1(q^2_{max})|^2, \tag{20}$$

while at opposite end of the heavy meson spectra, namely, at $q^2 = 0$ one obtains [7]

$$\frac{d\Gamma}{dy} = \frac{G_F^2 M_1^5}{96\pi^3}|V_{Q_1Q_2}|^2 \zeta(1-\zeta^2)^3 |A_0(0)|^2. \tag{21}$$

In the case of heavy–to–heavy transitions, in the limit in which the active quarks have infinite mass, all the form factors are given in terms of a single function $\xi(y)$, the Isgur–Wise form factor. In the realistic case of finite quark masses these relations are modified: each form factor depends separately on the dynamics of the process.

3 The matrix elements of the vector and axial currents

We determine all of the form factors by taking matrix elements of the plus components of the weak currents. Applying the standard LF technique for the time-like momentum transfer [3, 4] to the matrix element of the vector current $\bar{Q}_2\gamma^+ Q_1$ between two pseudoscalar mesons one obtains[1]

$$J_V(q^2, r) = < P_2|\bar{Q}_2\gamma^+ Q_1|P_1 > = \int_0^r \frac{dx}{x}\int d^2k_\perp \chi_2(x', k'^2_\perp)\chi_1(x, k^2_\perp)\cdot I_V, \tag{22}$$

where I_V is the contribution of the Dirac current and quark spin structure:

$$I_V = \mu_1\mu_2 Tr[R^+_{00}\bar{u}(\bar{p}_2, \lambda_2)\gamma^+ u(p_1, \lambda_1)R_{00}], \tag{23}$$

[1]The spectator quark carries the fraction x of the plus component of the meson momentum, while the heavy quark carries the fraction $1 - x$.

with

$$\mu_1 = [M_{10}^2 - (m_1 - m)^2]^{1/2}, \tag{24}$$

$$\mu_2 = [M_{20}^2 - (m_2 - m)^2]^{1/2}, \tag{25}$$

and

$$M_{10}^2 \equiv M_{10}^2(x, k_\perp^2) = \frac{m^2 + k_\perp^2}{x} + \frac{m_1^2 + k_\perp^2}{1 - x}, \tag{26}$$

$$M_{20}^2 \equiv M_{20}^2(x', k_\perp'^2) = \frac{m^2 + k_\perp'^2}{x'} + \frac{m_2^2 + k_\perp'^2}{1 - x'}. \tag{27}$$

In these equations m_1 and m_2 are the masses of active quarks, m is the mass of the quark–spectator, $x' = \frac{x}{r}$ and $\mathbf{k}'_\perp = \mathbf{k}_\perp + x'\mathbf{q}_\perp$. In our kinematics

$$k_1' = k_1 - x' q_\perp, \quad k_2' = k_2. \tag{28}$$

The spin wave functions R_{JJ_3} can be found in refs. [8, 9]. We choose a phenomenological wave function $\chi_i(x, k_\perp^2)$ by starting with the equal-time wave function $w_i(k^2)$ normalized according to

$$\int_0^\infty dk\ k^2\ w_i^2(k^2) = 1, \tag{29}$$

provided that the fraction x is replaced by the longitudinal momentum $k_3^{(1)}$ defined as

$$k_3^{(1)} = \left(x - \frac{1}{2}\right) M_{10} + \frac{m_1^2 - m^2}{2M_{10}}, \tag{30}$$

and the fraction x' is replaced by the longitudinal momentum $k_3^{(2)}$

$$k_3^{(2)} = \left(x' - \frac{1}{2}\right) M_{20} + \frac{m_2^2 - m^2}{2M_{20}}. \tag{31}$$

Explicitly, one has [3]

$$\chi_i(x, k_\perp^2) = \frac{1}{2(1-x)} \frac{\sqrt{M_{i0}[1 - (m_i^2 - m^2)^2/M_{i0}^4]}}{\sqrt{M_{i0}^2 - (m_i - m)^2}}\ \frac{w_i(k^2)}{\sqrt{4\pi}} \tag{32}$$

with $k^2 \equiv k_\perp^2 + k_3^2$. This procedure amounts to a series of reasonable (but naive) guesses about what the solution of a relativistic theory involving confining interactions might look like.

The matrix element of the vector current $\bar{Q}_2\gamma^+ Q_1$ between pseudoscalar and vector mesons is given by

$$J_V^{(+1)}(q^2, q_\perp) = < P_2 \varepsilon(+1) | \bar{Q}_2 \gamma^+ Q_1 | P_1 > = \int_0^{r(q^2, q_\perp)} \frac{dx}{x} \int d^2k_\perp \chi_2(x', k_\perp'^2) \chi_1(x, k_\perp^2) \cdot I_V^{(+1)}, \tag{33}$$

where

$$I_V^{(+1)} = \mu_1 \mu_2 [Tr R_{1+1}^+ \bar{u}(\bar{p}_2, \lambda_2) \gamma^+ u(p_1, \lambda_1) R_{00}] \tag{34}$$

To define the axial form factors we need two matrix elements of the axial current $\bar{Q}_2\gamma^+\gamma_5 Q_1$ corresponding to the transverse and longitudinal polarization states $\varepsilon(+1)$ and $\varepsilon(0)$ of a vector meson

$$J_A^{(+1)}(q^2,q_\perp) =< P_2\varepsilon(+1)|\bar{Q}_2\gamma^+\gamma_5 Q_1|P_1 >= \int\limits_0^{r(q^2,q_\perp)} \frac{dx}{x}\int d^2k_\perp \chi_2(x',k_\perp'^2)\chi_1(x,k_\perp^2)\cdot I_A^{(+1)}, \tag{35}$$

$$J_A^{(0)}(q^2,q_\perp) =< P_2\varepsilon(0)|\bar{Q}_2\gamma^+\gamma_5 Q_1|P_1 >= \int\limits_0^{r(q^2,q_\perp)} \frac{dx}{x}\int d^2k_\perp \chi_2(x',k_\perp'^2)\chi_1(x,k_\perp^2)\cdot I_A^{(0)}, \tag{36}$$

where

$$I_A^{(+1)} = \mu_1\mu_2 Tr[R^+_{1+1}\bar{u}(\bar{p}_2,\lambda_2)\gamma^+\gamma_5 u(p_1,\lambda_1)R_{00}], \tag{37}$$

$$I_A^{(0)} = \mu_1\mu_2 Tr[R^+_{10}\bar{u}(\bar{p}_2,\lambda_2)\gamma^+\gamma_5 u(p_1,\lambda_1)R_{00}]. \tag{38}$$

Noting that $\bar{u}(p_2,\lambda_2)\gamma^+u(p_1,\lambda_1) = \sqrt{4p_1^+p_2^+}\delta_{\lambda_2\lambda_1}$, $\bar{u}(p_2,\lambda_2)\gamma^+\gamma_5 u(p_1,\lambda_1) = \sqrt{4p_1^+p_2^+}\varphi^+_{\lambda_2}\sigma_3\varphi_{\lambda_1}$, where φ_λ are the Pauli spinors and using the explicit expressions for light-cone spin structure functions R_{JJ_3} from [8, 9] we obtain

$$I_V(x;r;k_\perp;q_\perp) = \frac{2M_1}{x'}[\mathcal{A}_1\mathcal{A}_2 + \mathbf{k}_\perp\mathbf{k}'_\perp], \tag{39}$$

$$I_V^{(+1)}(x;r;k_\perp;q_\perp) = -\frac{\sqrt{2}M_1}{x'}[k'_1\mathcal{A}_1 - k_1\mathcal{A}_2 + \frac{2k_2^2(k'_1-k_1)}{M_{20}+m+m_2}], \tag{40}$$

$$I_A^{(+1)}(x;r;k_\perp;q_\perp) = \frac{\sqrt{2}M_1}{x'}[(2x'-1)k'_1\mathcal{A}_1 + k_1\mathcal{A}_2 + 2k'_1\frac{\mathcal{A}_1\mathcal{B}+\mathbf{k}_\perp\mathbf{k}'_\perp}{M_{20}+m+m_2}], \tag{41}$$

$$I_A^{(0)}(x;r;k_\perp;q_\perp) = \frac{2M_1}{x'}[2x'(1-x')M_{20}\mathcal{A}_1 + \frac{(1-2x')M_{20}+m_2-m}{M_{20}+m+m_2}(\mathbf{k}_\perp\mathbf{k}'_\perp + \mathcal{A}_1\mathcal{B})], \tag{42}$$

with

$$\mathcal{A}_1 = xm_1 + (1-x)m, \quad \mathcal{A}_2 = x'm_2 + (1-x')m, \tag{43}$$

and

$$\mathcal{B} = (1-x')m - x'm_2. \tag{44}$$

4 The definition of the vector and axial form factors

We first reexamine an approach of ref. [3] to calculate the form factors $F_1(q^2)$ for the $PS-PS$ transitions. Eq. (6) for the plus component of the vector current yields only one constraint for the two form factors $F_1(q^2)$ and $F_0(q^2)$. In order to invert Eq. (6) the matrix element of the current was calculated in [3] in two reference frames having the 3-axis parallel and anti-parallel to the *3*-momentum of the daughter meson. This corresponds to the choice $\alpha_1 = 0, \alpha_2 = \pi$ where the angle α is defined in Section 2. One might ask what happens when we use two other frames. Specifying these frames by the two arbitrary angles α_1 and α_2 we can now write Eq. (35) of ref. [3] as

$$F_1(q^2) = \frac{(1-r(\alpha_2))J_V(q^2,r(\alpha_1)) - (1-r(\alpha_1))J_V(q^2,r(\alpha_2))}{2M_1(r(\alpha_1)-r(\alpha_2))}. \tag{45}$$

In this equation we can take the limit $\alpha_2 \to \alpha_1 = \alpha$ which would correspond to the use of only one reference frame specified by the angle α. In this case the form factor $F_1(q^2)$ is expressed in terms of the matrix element of the current and its derivative. Indeed, from Eq. (45) one derives

$$F_1(q^2) = \frac{1}{2M_1}\left[J_V(q^2, r(\alpha)) + (1 - r(\alpha))\frac{\partial J_V(q^2, r(\alpha))}{\partial r}\right]. \tag{46}$$

It is understood that when calculating the partial derivative $\frac{\partial J_V}{\partial r}$ the variable $q_\perp$ entering the integrand of Eq. (22) is expressed in terms of q^2 and r using Eq. (2).

The final choice of α can be made by the requirement that at the point of the maximum recoil, $q^2 = 0$, Eq. (46) must coincide with the standard LF result for $q^2 \leq 0$ obtained in the Breit frame [8, 9]. One can easily verify that this condition is fulfilled only for $\alpha = 0$. Eq. (46) for $\alpha = 0$ coincides with that of refs. [3, 4] at $q^2 = 0$ and $q^2 = q^2_{max}$, but the two definitions differ at intermediate q^2. Recall [3] that the time-like LF result for the "good" component of the weak vector current $J^+ = J^0 + J^3$ coincides with the contribution of the spectator pole of the Feynman triangle diagram, which corresponds to the valence quark approximation, while the remaining part of the Feynman diagram, the so-called Z graph, can not be expressed directly in terms of a valence quark wave function.[2] The sum of both contributions does not depend, of course, on the choice of the frame but each contribution is frame-dependent. Therefore the time-like LF result for the form factors generally depends on the recoil direction of the daughter meson relative to the 3-axis e.g. on the choice of angles α specifying a reference frame. Fortunately this dependence is marginal even for heavy-to-light transitions. We shall illustrate this point later on.

Now we apply the same procedure to the calculation of the form factors governing the $PS - V$ transitions. The vector form factor $V(q^2)$ can be found from Eqs. (7, 33). Note that for the pure longitudinal configuration both the integral of Eq. (33) and the covariant

$$\varepsilon_{+\nu\alpha\beta}\varepsilon^{*\nu}(+1)P_1^\alpha P_2^\beta = -\frac{i}{\sqrt{2}}M_1 M_2\sqrt{y^2-1}\sin\alpha \equiv -\frac{i}{\sqrt{2}}M_1 q_\perp \tag{47}$$

vanish. Therefore to calculate the form factor $V(q^2)$ we will choose $\alpha \neq 0$ at the outset and let $\alpha \to 0$ at the end of calculations to get

$$V(q^2) = \frac{1}{\sqrt{2}}(1+\zeta)\left[\frac{\partial}{\partial q_\perp}J_V^{(+1)}(q^2, q_\perp)\right]_{q_\perp=0}. \tag{48}$$

To define the axial form factors we first note that

$$J_A^{(+1)} = \frac{1}{\sqrt{2}}M_1 q_\perp\left(\frac{1+r(\alpha)}{r(\alpha)}a_+(q^2) + \frac{1+r(\alpha)}{r(\alpha)}a_-(q^2)\right). \tag{49}$$

Then we proceed exactly in the same way as was described above for calculating the form factor $F_1(q^2)$. An additional difficulty is that the integral of Eq. (35) also vanishes for $\alpha = 0$. Therefore to invert Eq.(35) we first solve it for $\alpha = \alpha_1$ and $\alpha = \alpha_2$ and then take the limit $\alpha_1, \alpha_2 \to 0$. We obtain

$$a_\pm(q^2) = \pm\frac{1}{\sqrt{2}M_1}\left(A^{(+)}(r) + r(1 \mp r)\frac{dA^{(+)}(r)}{dr}\right), \tag{50}$$

[2] Note that the contribution of the Z-graph is expressed in terms of the integral over the region $r \leq x \leq 1$, therefore to diminish its contribution one must choose r (at given q^2) to have its maximum close to 1; in this way we again come to the choice $\alpha = 0$.

where

$$A^{(+)}(r) = \left[\frac{\partial}{\partial q_\perp} J_A^{(+1)}(q^2, q_\perp)\right]_{q_\perp=0}. \tag{51}$$

In order to calculate the remaining form factor $f(q^2)$ we use the longitudinal polarization $\varepsilon(0)$ [8] to get

$$f(q^2) = -\frac{\zeta}{r}\left[J_A^{(0)}(q^2, q_\perp) + \frac{M_2}{\sqrt{2}\zeta^2}(r^2 - \zeta^2)A^{(+)}(r)\right]_{q_\perp=0}. \tag{52}$$

At the point of the maximum recoil one obtains from Eqs. (48), (50) and(52)

$$V(0) = \frac{1}{\sqrt{2}}(1+\zeta)\left[\frac{d}{dq_\perp} J_V^{(+1)}(0, q_\perp)\right]_{q_\perp=0}, \tag{53}$$

$$A_0(0) = \frac{1}{2M_1} J_A^{(0)}(0,0), \tag{54}$$

and

$$A_2(0) = \frac{1+\zeta}{\sqrt{2}}\left[\frac{d}{dq_\perp} J_A^{(+1)}(0, q_\perp)\right]_{q_\perp=0}, \tag{55}$$

where the relationships (13, 15) between the form factors A_0, A_2 and the form factors $a_\pm$ and f have been used. We show in the Appendix that Eqs. (53-55) coincide with the standard result [8, 9] obtained using the Hamiltonian LF formalism in the Breit frame[3].

5 Results

The calculation of the semileptonic form factors $F_1(q^2)$, $V(q^2)$, $A_0(q^2)$, $A_1(q^2)$ and $A_2(q^2)$ has been performed using our LF results (Eqs. 46, 48, 50, 52) for computing the matrix elements of the vector and axial weak currents. The LF meson wave functions χ_i are constructed according to the rules given in Section 3. For the radial wave functions appearing in Eq. (32), the Gaussian ansatz of the ISGW model has been adopted in which the main characteristic is confinement[4]. The values of the parameters are taken from the updated version [11] of the ISGW model[5]. We use the physical values for the meson masses taken from the latest Particle Data Group publication [13].

Our results for the form factors at $q^2 = 0$ and semileptonic decay rates Γ (Eqs. (16, 17)) are collected in Tables 1 and 2. The q^2 behavior of the form factors $F_1(q^2)$ for $B \to D\ell\nu_\ell$, $B \to \pi\ell\nu_\ell$, $D \to K\ell\nu_\ell$, and $D \to \pi\ell\nu_\ell$ semileptonic transitions is shown in Figs. 1–4, respectively, while the q^2 behavior of the form factors $V(q^2)$, $A_0(q^2)$, $A_1(q^2)$, and $A_2(q^2)$ for $B \to D^*\ell\nu_\ell$, $B \to \rho\ell\nu_\ell$, $D \to K^*\ell\nu_\ell$, and $D \to \rho\ell\nu_\ell$ transitions is shown in Figs. 5–8. Note that near the zero-recoil point $y = 1$ the form factors do not obey at all the pattern of pole dominance and even may have a negative slope. This behavior, especially prominent for the $b \to u$ transitions, can be ascribed to the fact that our

[3]We have compared our numerical results for the $PS \to V$ form factors with those of Jaus [10] using the set of quark model parameters (the constituent quark masses and harmonic oscillator lengths) found in [10] by exploiting the duality of the VMD and CQM pictures. This comparison is presented in Table 1. Note that there is a misprint in Table VI of ref. [10]. The correct Table is obtained if the symbols V, A_1 and A_2 are replaced by A_1, A_2, and V . Our results for the vector and axial form factors for B and D decays are very similar to the results of ref. [10] but the rates are a bit different and reflect the difference in the q^2 dependence of the form factors.

[4]There is some model dependence here; other choices [4] for $w(k^2)$ will lead for somewhat different predictions.

[5]In what follows this updated version will be referred as the ISGW2 model.

calculations do not include the contribution of the quark-pair creation diagram (the Z-graph) which, in another language, corresponds to the contribution of $|B^*\pi>$ or $|D^*\pi>$ states [14]. However, the corresponding decay rates are not affected by the Z-graph because the contribution to the rates arising from the region near $y = 1$ is kinematically suppressed.

In order to estimate uncertainties introduced by a particular choice of the reference frame we have compared in Table 2 the decay rates for the $PS - PS$ transitions calculated from our new Eq. (46) (corresponding to the choice $\alpha_1, \alpha_2 \to 0$) and from Eq. (35) of ref. [3] (corresponding to the choice $\alpha_1 = 0, \alpha_2 = \pi$). We have found the new decay rates to be slightly smaller than those of ref. [3]: the differences comprise 7% for $b \to c$, 9% for $b \to u$, 13% for $c \to s$, and 4% for $c \to u$ transitions. We conclude that a good stability of the results is always maintained and the decay rates (with exception of $c \to s$ case) are predicted with accuracy better than 10%. The same conclusion is preserved for more complicated meson wave functions corresponding to the inclusion of the one-gluon exchange at small distances [12].

We now discuss the results arranged in order of decreasing active quark mass. We will compare our results to experimental data and to predictions of different models.

5.1 Decays $B \to D\ell\nu_\ell$ and $B \to D^*\ell\nu_\ell$

First, we want to estimate the values of $|V_{cb}|$ based on our predictions of the normalization of the form factors and their q^2 dependence. From the partial widths[6]

$$\Gamma(B^0 \to D^-\ell^+\nu_\ell) = (1.22 \pm 0.32) \cdot 10^{10}\ s^{-1}, \tag{56}$$

$$\Gamma(B^0 \to D^{-*}\ell^+\nu_\ell) = (2.92 \pm 0.17) \cdot 10^{10}\ s^{-1} \tag{57}$$

and our predicted rates for $\Gamma(B^0 \to D^-\ell^+\nu_\ell)$ and $\Gamma(B^0 \to D^{*-}\ell^+\nu_\ell)$ from Table 2, we obtain

$$|V_{bc}| = 0.037 \pm 0.004, \quad (B^0 \to D^-\ell^+\nu_\ell), \tag{58}$$

$$|V_{bc}| = 0.036 \pm 0.002, \quad (B^0 \to D^{-*}\ell^+\nu_\ell). \tag{59}$$

The results are consistent in that the extracted values of V_{bc} are consistent for two decay modes. Fig.9 shows the $\frac{d\Gamma}{dq^2}$ distribution calculated for $|V_{bc}| = 0.036$ and $|V_{bc}| = 0.0374$. The last value has been obtained from our fit to the recent CLEO data [16]. Both LF predictions are in agreement with the updated "experimental" determinations of $|V_{bc}|$ [19] obtained from exclusive and inclusive semileptonic decays of the B-meson ($|V_{bc}|_{excl} = 0.0373 \pm 0.0045_{exp} \pm 0.0065_{th}$ and $|V_{bc}|_{incl} = 0.0398 \pm 0.0008_{exp} \pm 0.0040_{th}$), and also agree within the error bars with the recent determination $|V_{bc}| = 0.041 \pm 0.003 \pm 0.002$ from a partial rate $\frac{d\Gamma(B\to D^*\ell\nu_\ell)}{dy}$ corresponding to the kinematical region where D^* recoil slowly [15]. In Table 3 we compare the values of $|V_{bc}|$ for several quark models.

Our predicted values $R_1 = V(0)/A_1(0) = 1.08$ and $R_2 = A_2(0)/A_1(0) = 0.89$ are in good agreement with the preliminary fit results by CLEO [18] $R_1 = 1.18 \pm 0.30 \pm 0.12$ and $R_2 = 0.71 \pm 0.22 \pm 0.07$. For the branching ratios $BR(B^0 \to D^-\ell^+\nu_\ell)$, $BR(B^0 \to D^{*-}\ell^+\nu_\ell)$ we obtain

$$BR(B^0 \to D^-\ell^+\nu_\ell) = 2.12 \left|\frac{V_{cb}}{0.039}\right|^2, \tag{60}$$

[6]These values have been derived by combining the branching ratios $Br(B^0 \to D^-\ell^+\nu_\ell) = (1.9 \pm 0.5)\%$ and $Br(B^0 \to D^{-*}\ell^+\nu_\ell) = (4.56 \pm 0.27)\%$ with the world average of the B^0 lifetime $\tau_{B^0} = 1.56 \pm 0.06\ ps$ [13]. Our estimation of $\Gamma(B^0 \to D^{-*}\ell^+\nu_\ell)$ agrees with the recent result by CLEO collaboration [16] $\Gamma(B^0 \to D^{-*}\ell^+\nu_\ell) = [2.99 \pm 0.19(stat) \pm 0.27(syst) \pm 0.20(lifetime)] \cdot 10^{10}\ s^{-1}$ based on the average of the LEP and CDF measurements of the lifetimes [17], $\tau_{B^0} = 1.53 \pm 0.09\ ps$, $\tau_{B^+} = 1.68 \pm 0.12\ ps$.

$$BR(B^0 \to D^{*-}\ell^+\nu_\ell) = 5.40 \left|\frac{V_{cb}}{0.039}\right|^2. \tag{61}$$

These values only slightly exceed the corresponding branching fractions obtained using the heavy-quark symmetry approximation i.e. adopting a single Isgur-Wise function for all the form factors: $BR(B^0 \to D^-\ell^+\nu_\ell) = 1.65 \left|\frac{V_{cb}}{0.039}\right|^2$, and $BR(B^0 \to D^{*-}\ell^+\nu_\ell) = 5.17 \left|\frac{V_{cb}}{0.039}\right|^2$. Our prediction for the ratio of of the longitudinal and transversal contributions to the $B \to D^*$ decay is 1.17 which agrees with the recent result by CLEO Collaboration $\frac{\Gamma_L}{\Gamma_T} = 1.24 \pm 0.16$ [33]. We also obtain the ratio

$$\frac{\Gamma(B^0 \to D^{*-}\ell^+\nu_\ell)}{\Gamma(B^0 \to D^-\ell^+\nu_\ell)} = 2.54, \tag{62}$$

that agrees with experimental result 2.4 ± 0.6 [13]. Some other model predictions for the $B \to D^*$ decay are collected in Table 4.

5.2 Decays $B \to \pi\ell\nu_\ell$ and $B \to \rho\ell\nu_\ell$

We now consider the semileptonic B-meson decay corresponding to the quark process $b \to u\ell\nu_\ell$. The investigation of this decay is very important for the determination of the CKM matrix element $|V_{bu}|$, which plays an important role for the CP violation in the Standard Model. The determination of V_{bu} is one of the most challenging measurements in B physics. Very recently, the CLEO Collaboration [20] has reported the first signal for exclusive semileptonic decays of the B meson into charmless final states, in particular for the decay modes $B \to \pi\ell\nu_\ell$, $B \to \rho\ell\nu_\ell$. However, there is a significant model dependence in the simulation of the reconstruction efficiencies. The observed branching ratios, assuming the efficiencies obtained from the ISGW model [22] are

$$Br(B \to \pi\ell\nu_\ell) = (1.34 \pm 0.45) \cdot 10^{-4}, \quad Br(B \to \rho\ell\nu_\ell) = (2.28^{+0.69}_{-0.83}) \cdot 10^{-4}. \tag{63}$$

From our predicted rates $\Gamma(B^0 \to \pi^-\ell^+\nu_\ell) = 8.72\ |V_{bu}|^2\ ps^{-1}$ and $\Gamma(B^0 \to \rho^-\ell^+\nu_\ell) = 13.2\ |V_{bu}|^2\ ps^{-1}$ (see Table 2) we obtain

$$|V_{bu}| = 0.0031 \pm 0.0004, \quad (B^0 \to \pi^-\ell^+\nu_\ell), \tag{64}$$

$$|V_{bu}| = 0.0033 \pm 0.0004, \quad (B^0 \to \rho^-\ell^+\nu_\ell). \tag{65}$$

Using our previous result, Eqs.(58, 59), for $|V_{bc}|$ we get

$$\left|\frac{V_{bu}}{V_{cb}}\right| = 0.087 \pm 0.015, \quad (B^0 \to \pi^-\ell^+\nu_\ell), \tag{66}$$

$$\left|\frac{V_{bu}}{V_{cb}}\right| = 0.092 \pm 0.015, \quad (B^0 \to \rho^-\ell^+\nu_\ell). \tag{67}$$

These values are in agreement[7] with the value derived from measurements of the end-point region of the lepton spectrum in inclusive semileptonic decays [24, 25] viz.

$$\left|\frac{V_{bu}}{V_{cb}}\right|_{incl} = 0.08 \pm 0.01_{exp} \pm 0.02_{th}. \tag{68}$$

[7] If the BSW model [23] is used to reconstruct efficiencies the branching fractions are somewhat higher: $Br(B \to \pi\ell\nu_\ell) = (1.63 \pm 0.57) \cdot 10^{-4}$, and $Br(B \to \rho\ell\nu_\ell) = (3.88^{+1.15}_{-1.39}) \cdot 10^{-4}$. Combining the average of experimental results for the ISGW and BSW models with our predicted rates one obtains $|V_{bu}| = 0.0033 \pm 0.0004$, $\left|\frac{V_{bu}}{V_{cb}}\right| = 0.092 \pm 0.015$, $(B^0 \to \pi^-\ell^+\nu_\ell)$ and $|V_{bu}| = 0.0039 \pm 0.0004$, $\left|\frac{V_{bu}}{V_{cb}}\right| = 0.107 \pm 0.015$, $(B^0 \to \rho^-\ell^+\nu_\ell)$.

A large variety of calculations of the ratio $|V_{bu}/V_{bc}|$, based on various non-perturbative approaches, exists in the literature; the results typically lie in the range from 0.06 to 0.11. A sample of these calculations is given in Table 5.

Note that our result for the ratio of branching fractions

$$\frac{\Gamma(B^0 \to \rho^- \ell^+ \nu_\ell)}{\Gamma(B^0 \to \pi^- \ell^+ \nu_\ell)} = 1.51 \tag{69}$$

compares favorably to the recent CLEO result [20]:

$$\frac{\Gamma(B^0 \to \rho^- \ell^+ \nu_\ell)}{\Gamma(B^0 \to \pi^- \ell^+ \nu_\ell)} = 1.70^{+0.80}_{-0.30} \pm 0.58^{+0.00}_{-0.34} \tag{70}$$

The dispersion relation approach to the ISGW2 model [21] yields for this ratio the values of $1.17-1.34$. Our prediction for the ratio Γ_L/Γ_T for the $B \to \rho\ell\nu_\ell$ decay rate is 0.92; other models yield $\Gamma_L/\Gamma_T =$ 1.13 [21], 1.34 [23], 0.3 [11], 0.82 [10], and 0.52 ± 0.08[31].

5.3 Decays $D \to K\ell\nu_\ell$ and $D \to K^*\ell\nu_\ell$

In the charm sector, the absolute scale of theoretical predictions for the form factors which characterize the hadronic $D \to K^*$ and $D \to \rho$ matrix elements of the weak currents can be tested, because the CKM elements can be determined independently of the D semileptonic decay rate using the assumption of CKM unitarity and the smallness of the CKM matrix elements for B decay [30]. Semileptonic decays $D \to K^*\ell\nu_\ell,\ \ell = e, \mu$ have been studied extensively and the form factors have been determined (with some assumptions concerning their shape). In particular, the CLEO collaboration [29] has measured all four $D \to K(K^*)\ell\nu_\ell$ decays in one experiment:

$$\Gamma(D \to K\ell\nu_\ell) = (9.1 \pm 0.3 \pm 0.6) \cdot 10^{10} s^{-1}, \tag{71}$$

$$\Gamma(D \to K^* l\nu_l) = (5.7 \pm 0.7) \cdot 10^{10} s^{-1}, \tag{72}$$

$$R = \frac{\Gamma(D \to K^* l\nu_l)}{\Gamma(D \to K\ell\nu_\ell)} = 0.62 \pm 0.08. \tag{73}$$

Using $|V_{cs}| = 0.974$ we predict

$$\Gamma(D \to K\ell\nu_\ell) = 9.38 \cdot 10^{10} s^{-1}, \tag{74}$$

$$\Gamma(D \to K^*\ell\nu_\ell) = 6.36 \cdot 10^{10} s^{-1}, \tag{75}$$

$$R = 0.68, \tag{76}$$

in an agreement with experimental data. Some other model predictions for the $D \to K^*$ decay are collected in Table 6.

5.4 Decays $D \to \pi\ell\nu_\ell$ and $D \to \rho\ell\nu_\ell$

Assuming $|V_{cd}| = 0.221$, which is inferred from the unitarity of the CKM matrix [13], we predict for the semileptonic decay rates the following values:

$$\Gamma(D^0 \to \pi^- e^+ \nu_e) = 7.4 \cdot 10^{-3}\ ps^{-1}, \tag{77}$$

$$\Gamma(D^0 \to \rho^- e^+ \nu_e) = 3.8 \cdot 10^{-3}\ ps^{-1}. \tag{78}$$

These predictions should be compared with the experimental result

$$\Gamma_{exp}(D^0 \to \pi^- e^+ \nu_e) = (9.4^{+5.5}_{-2.9}) \cdot 10^{-3}\ ps^{-1}, \tag{79}$$

and the recent light-front QCD sum rule prediction [26].

$$\Gamma_{SR}(D^0 \to \pi^- e^+ \nu_e) = (7.6 \pm 0.2) \cdot 10^{-3}\ ps^{-1}. \tag{80}$$

The CLEO collaboration [27] recently determined the following ratio of decay rates

$$\frac{\Gamma(D^0 \to \pi^- e^+ \nu_e)}{\Gamma(D^0 \to K^- e^+ \nu_e)} = 0.103 \pm 0.039 \pm 0.013, \tag{81}$$

while the $E653$ collaboration [28] measured

$$\frac{\Gamma(D^0 \to \rho^- e^+ \nu_e)}{\Gamma(D^0 \to K^{*-} e^+ \nu_e)} = 0.088 \pm 0.062 \pm 0.028. \tag{82}$$

Our calculated fractions are 0.079 and 0.060, respectively, which seem to be a bit small; nevertheless they are in agreement with the experimental values within the large error bars. The dispersion approach to the ISGW2 model [21] yields for these fractions 0.071 and $0.047 - 0.056$.

6 Conclusions

In this paper we have examined the weak transition form factors which govern the heavy-to-heavy and heavy-to-light semileptonic decays of pseudoscalar mesons within a relativistic constituent quark model based on the light-front formalism. We have obtained all the relevant expressions for the weak vector and axial form factors. For numerical estimates we employed the LF wave function, that is related to the equal-time wave function of the ISGW model. The transition form factors have been calculated in the whole kinematical region accessible in semileptonic decays. We have calculated the form factors and the decay rates for the $B \to D(D^*)\ell\nu_\ell$, $B \to \pi(\rho)\ell\nu_\ell$, $D \to K(K^*)\ell\nu_\ell$ and $D \to \pi(\rho)\ell\nu_\ell$ semileptonic decays. Our results have been successfully compared with available experimental data. In particular for $b \to c$ and $b \to u$ transitions, using the available experimental information on the semileptonic decay rates, the CKM parameters have been estimated.

Since our calculations neglect the contribution of the pair creation from the vacuum it would appear that the good agreement with the data suggests that these might very well be small. However, an estimate of such contributions, particularly in case of the heavy-to-light transitions, is important for there to be a complete comparison with experimental data.

Acknowledgment

We thank I.L. Grach for the collaboration in the early stages of this work. The authors acknowledge the financial support of the INTAS–RFBR grant, ref. No 95–1300. This work was in part supported by the RFBR grant, ref. No 95-02-04808a and by the Natural Sciences and Engineering Council of Canada.

Appendix. Form factors at $q^2 = 0$

In this Appendix we show that Eqs. (53-55) for $V(0)$, $A_0(0)$ and $A_2(0)$ coincide with the ones obtained using the LF formalism in the Breit frame for $q^2 \leq 0$. Using our notation we write[8] Eqs.(4.4, 4.5, 4.6a, 4.9) of Ref. [8] in the form

$$V(q^2) = \frac{M_1 + M_2}{\sqrt{2}M_1} \int_0^1 \frac{dx}{x} \int d^2k_\perp \chi_2(x, k'^2_\perp)\chi_1(x, k^2_\perp)\mathcal{I}_V^{(+1)}(x; k_\perp; q_\perp), \tag{A.1}$$

$$A_0(q^2) = \frac{1}{2M_1} \int_0^1 \frac{dx}{x} \int d^2k_\perp \chi_2(x, k'^2_\perp)\chi_1(x, k^2_\perp)\mathcal{I}_A^{(0)}(x; k_\perp; q_\perp), \tag{A.2}$$

$$A_2(q^2) = \frac{M_1 + M_2}{\sqrt{2}M_1} \int_0^1 \frac{dx}{x} \int d^2k_\perp \chi_2(x, k'^2_\perp)\chi_1(x, k^2_\perp)\mathcal{I}_A^{(+1)}(x; k_\perp; q_\perp), \tag{A.3}$$

where

$$\mathcal{I}_V^{(+1)}(x; k_\perp; q_\perp) = \sqrt{2}M_1 \left[\mathcal{A}_1 - \frac{m_1 - m_2}{q^2}\mathbf{k}_\perp\mathbf{q}_\perp + \frac{2}{M_{20} + m_2 + m}\left[k^2_\perp + \frac{(\mathbf{k}_\perp\mathbf{q}_\perp)^2}{q^2}\right]\right], \tag{A.4}$$

$$\mathcal{I}_A^{(0)}(x; k_\perp; q_\perp) = 2M_1 \left[2(1-x)M_{20}\mathcal{A}_1 + \frac{(1-2x)M_{20} + m_2 - m}{x(M_{20} + m_2 + m)}(\mathbf{k}_\perp\mathbf{k}'_\perp + \mathcal{A}_1\mathcal{B})\right], \tag{A.5}$$

$$\mathcal{I}_A^{(+1)}(x; k_\perp; q_\perp) = -\sqrt{2}M_1 \left[(2x-1)\mathcal{A}_1 - \right.$$
$$\left. \frac{\mathbf{k}_\perp\mathbf{q}_\perp}{q^2}[2(1-x)m + m_2 + (2x-1)m_1] + 2\frac{1 - \frac{\mathbf{k}_\perp\mathbf{q}_\perp}{xq^2}}{M_{20} + m_2 + m}(\mathbf{k}_\perp\mathbf{k}'_\perp + \mathcal{A}_2\mathcal{B})\right], \tag{A.6}$$

and $\mathbf{k}'_\perp = \mathbf{k}_\perp + x\mathbf{q}_\perp$.

Noting that in our kinematics the momentum transfer is anti-parallel to the 1-axis, i.e., $q = (q^0, q^1, q^2, q^3) = (0, -q_\perp, 0, 0)$ we obtain after simple algebra

$$\mathcal{I}_V^{(+1)}(x; k_\perp; q_\perp) = \frac{1}{q_\perp} I_V^{(+1)}(x, 1, k_\perp, q_\perp), \tag{A.7}$$

$$\mathcal{I}_A^{(0)}(x; k_\perp; q_\perp) = I_A^{(0)}(x; 1; k_\perp; q_\perp), \tag{A.8}$$

$$\mathcal{I}_A^{(+1)}(x; k_\perp; q_\perp) = \frac{1}{q_\perp} I_A^{(+1)}(x; 1; k_\perp; q_\perp), \tag{A.9}$$

In the limit $q_\perp \to 0$ using Eqs. (33, 35, 36) one easily derives that Eqs. (A.1, A.2, A.3) coincide with Eqs. (53, 54, 55).

[8]Note that our variables and notation are related to those of ref. [8] by

$$\mathbf{p}''_\perp = -\mathbf{k}'_\perp, \quad \mathbf{p}'_\perp = -\mathbf{k}_\perp, \quad \xi = 1 - x, \quad m_2 = m, \quad m''_1 = m_2, \quad m'_1 = m_1,$$

The quantity $\Omega(p'', p')$ defined by Eq.(4.2) of [8] can be written in terms of our LF functions as

$$\frac{dk_3}{dx}\frac{1}{1-x}\Omega(k', k) = \frac{1}{x}\chi_2(x, k'^2_\perp)\chi_1(x, k^2_\perp)$$

Table 1. Form factors at $q^2 = 0$ and decay rates for the set of quark model parameters of [10]. The decay rates for bc and bu transitions are in the units $|V_{bc}|^2 ps^{-1}$ and $|V_{bu}|^2 ps^{-1}$, respectively. The decay rates for cs and cd transitions are in units $10^{10} s^{-1}$. The values of the CKM parameters $|V_{cd}| = 0.22$, $|V_{cs}| = 0.9743$ are used. In parentheses are given the numerical results of ref. [10].

Q_1Q_2	$F_1(0)$	$V(0)$	$A_1(0)$	$A_2(0)$	$\Gamma(PS \to PS)$	$\Gamma(PS \to V)$
bc	0.68(0.69)	0.79(0.81)	0.67(0.69)	0.61(0.64)	9.3(9.6)	24.5(25.3)
bu	0.25(0.27)	0.34(0.35)	0.26(0.26)	0.24(0.24)	8.1(10)	18.3(19.1)
cs	0.78(0.78)	1.03(1.04)	0.65(0.66)	0.43(0.43)	9.7(9.6)	6.2(5.5)
cd	0.66(0.67)	0.90(0.93)	0.57(0.58)	0.42(0.42)	0.7(0.8)	0.39(0.33)

Table 2. Form factors at $q^2 = 0$ and decay rates for the set of quark model parameters of [11]. The decay rates for bc and bu transitions are in the units $|V_{bc}|^2 ps^{-1}$ and $|V_{bu}|^2 ps^{-1}$, respectively. The decay rates for cs and cu transitions are in $|V_{cs}|^2 10^{10} s^{-1}$ and $|V_{cd}|^2 10^{10} s^{-1}$, respectively. In parentheses are given the decay rates for the $PS - PS$ transitions taken from ref. [3].

Q_1Q_2	$F_1(0)$	$V(0)$	$A_1(0)$	$A_2(0)$	$A_0(0)$	$\Gamma(PS \to PS)$	$\Gamma(PS \to V)$
bc	0.683	0.677	0.623	0.556	0.678	9.09(9.78)	23.10
bu	0.293	0.216	0.170	0.155	0.214	8.72(9.62)	13.2
cs	0.780	0.777	0.633	0.464	0.73	9.88(11.30)	6.70
cd	0.681	0.663	0.502	0.366	0.60	15.29(16.0)	7.85

Table 3. Model-dependent predictions of the $\bar{B} \to D^* \ell \bar{\nu}$ partial width V_{cb} values derived from the measured partial width. An additional 3.5% systematic error due to B lifetime measurements is common to all the $|V_{cb}|$ values given.

	This work	ISGW[22]	BSW[23]	KS[40]
$\Gamma(\bar{B} \to D^* \ell \bar{\nu})\|V_{cb}\|^{-2}$	$23.1 ps^{-1}$	$24.6 ps^{-1}$	$21.9 ps^{-1}$	$25.8 ps^{-1}$
$10^3 \cdot \|V_{cb}\|$	$35.6 \pm 1.1 \pm 1.6$	$34.8 \pm 1.1 \pm 1.6$	$37.5 \pm 1.2 \pm 1.7$	$34.4 \pm 1.1 \pm 1.5$

Table 4. Form factors at $q^2 = 0$ and the decay widths in for the semileptonic $B^0 \to D^*$ transition. The model predictions for the width are in $|V_{bc}|^2\ ps^{-1}$.

$B \to D, D^*$	$V(0)$	$V(0)/A_1(0)$	$A_2(0)/A_1(0)$	$\Gamma(D^*)$	$\Gamma(D)/\Gamma(D^*)$	Γ_L/Γ_T
This work	0.68	1.08	0.89	23.1	0.38	1.15
DR[21]	0.68	1.08	0.89	21.0	0.41	1.28
ISGW2[11]				24.8	0.48	1.04
KS[40]		1.54	1.39	25.8	0.32	
BSW[23]	0.71	1.09	1.06	22.0	0.36	
Stech [32]	0.75	1.10	1.02	24	0.37	
SR [35]	0.58	1.26 ± 0.08	1.15 ± 0.20	17 ± 6	0.53 ± 0.11	
Exp. [18],[33]		$1.18 \pm 0.30 \pm 0.12$	$0.71 \pm 0.22 \pm 0.07$		0.46 ± 0.2	1.24 ± 0.16

Table 5. Values for $|\frac{V_{ub}}{V_{cb}}|$ extracted from CLEO measurement of exclusive semileptonic B decays into charmless final states. Following Neubert [34] we take in this comparison $|V_{cb}| = 0.040$. An average over the experimental results obtained using the ISGW and BSW models to reconstruct efficiencies is used for all except the ISGW and BSW models, where the numbers corresponding to these models are used. For our LF model we use the values quoted in Eq.(64, 65). The first error quoted is experimental, the second (when available) is theoretical. For the recent LC SR result [31] only the theoretical error is quoted.

Method	Reference	$\bar{B} \to \pi \ell \bar{\nu}$	$\bar{B} \to \rho \ell \bar{\nu}$
LF QM	this work	0.078 ± 0.013	$0.083^{+0.013}_{-0.015}$
QCD sum rules	Narison [35]	$0.159 \pm 0.019 \pm 0.001$	$0.066^{+0.007}_{-0.009} \pm 0.003$
	Ball [31]		0.086 ± 0.013
	KhR [26]	0.085 ± 0.010	
Lattice QCD	UKQCD[37]	$0.103 \pm 0.012^{+0.012}_{-0.010}$	
	APE [38]	$0.084 \pm 0.010 \pm 0.021$	
pQCD	Li and Yu [39]	0.054 ± 0.006	
Quark models	BSW [23]	0.093 ± 0.016	$0.076^{+0.011}_{-0.014}$
	KS [40]	0.088 ± 0.011	$0.056^{+0.006}_{-0.007}$
	ISGW2 [11]	0.074 ± 0.012	$0.079^{+0.012}_{-0.014}$

Table 6. Form factors at $q^2 = 0$ and the decay widths in 10^{10} s^{-1} for the semileptonic $D^0 \to K^*$ transition. For our calculations we use $|V_{cs}| = 0.974$

$D^0 \to K^*$	$V(0)$	$A_1(0)$	$A_2(0)$	$\Gamma(K^*)$	Γ_L/Γ_T
This work	0.777	0.633	0.464	6.36	1.30
DR [21]	0.777	0.633	0.464	5.38	1.31
SR [36]	1.1 ± 0.25	0.50 ± 0.15	0.60 ± 0.15	3.8 ± 1.5	0.86 ± 0.06
Lat. [38]	1.08 ± 0.22	0.67 ± 0.11	0.49 ± 0.34	6.9 ± 1.8	1.2 ± 0.3
Lat. [37]	$1.01^{+0.3}_{-0.13}$	$0.70^{+0.07}_{-0.10}$	$0.60^{+0.10}_{-0.15}$	$6.0^{+0.8}_{-1.6}$	1.06 ± 0.16
Stech [32]	1.07	0.69	0.73	7.1	0.97
Exp. [13]	1.1 ± 0.2	0.56 ± 0.04	0.40 ± 0.08	5.7 ± 0.7	1.15 ± 0.17

References

[1] For a review see M.Neubert, Phys. Rep. **245** (1994) 259.

[2] For the literature on quark models see
D.Melikhov, Phys. Rev. **D53** (1996) 2460; Phys. Lett. **380** (1996) 363;
R.N.Faustov et al., Phys. Rev. **D53** (1996) 6302;
M.A.Ivanov and Y.M.Valit, hep–ph/9606404;
H.Y.Cheng *et al.*, hep–ph/9607332.

[3] N.B.Demchuk, I.L.Grach, I.M.Narodetskii and S.Simula, Yad. Phys. **59** (1996) 2235.

[4] I.L.Grach, I.M.Narodetskii and S.Simula, Phys.Lett. **B385** (1996) 317.

[5] M.V. Terent'ev, Yad.Fiz. **24** 207 [Sov. J. Nucl. Phys. **24** (1976) 106]; V.B. Berestetsky and M.V. Terent'ev, Yad.Fiz. **24** (1976) 1044 [Sov. J. Nucl. Phys **24** (1976) 547].

[6] C.O. Dib and F. Fera, Phys. Rev. **D47** (1993) 3938.

[7] P.J.O'Donnell and G.Turan, UTPT-96-6.

[8] W.Jaus, Phys. Rev. **D41** (1990) 3394.

[9] P.J.O'Donnell, Q.P.Xu and H.K.K.Tung, Phys. Rev. **D52** (1995) 3966.

[10] W.Jaus, Phys. Rev. **D53** (1996) 1349, and private communication.

[11] D.Scora, N.Isgur, Phys. Rev. **D52** (1995) 2783.

[12] I.L.Grach, private communication.

[13] Particle Data Group, R.M.Barnet *et al*, Phys. Rev. **D53** (1996) 1.

[14] N.Isgur, M. Wise, Phys. Rev **D41** (1990) 151.

[15] J.D.Richman, ref.[13], p.482.

[16] CLEO Collaboration: B.Barish *et al.*, Phys. Rev. **D51** (1995) 1014.

[17] W.Venus, in *Lepton and Photon Interactions*, Proceedings of the XVI International Symposium, Ithaca, New York, 1993, edited by P.Drell and D.Rubin, AIP Conf. Proc. No 302 (AIP, New York, 1994).

[18] J.Gronberg *et al.* CLEO preprint CLEO–CONF–95–27 (1995).

[19] T.Skwarnicki, in Proceedings of the 17^{th} International Symposium on Lepton-Photon Interactions, Beijing (China), August 1995, eds. Z. Zhi-Peng and C. He-Sheng (World Scientific, Singapore, 1996), p.238

[20] R.Ammar et al. CLEO-CNF 95-09 (1995) [eps0165].

[21] D.Melikhov, hep-ph/9611364.

[22] N. Isgur, G. Scora, B. Grinstein, M. Wise, Phys. Rev. **D39** (1989) 799.

[23] M.Wirbel, B.Stech, and M.Bauer, Z. Phys. **C29** (1985) 637.

[24] ARGUS Collaboration, H. Albrecht *et al.* Phys. Lett. **B255** (1991) 297.

[25] CLEO Collaboration, J.Bartelt *et al.* Phys. Rev. Lett. **71** (1993) 4111.

[26] A.Khodjamirian and R.Rückl Nucl. Instr. and Meth. **A368** (1995) 28.

[27] CLEO Collaboration, F.Butler *et al.* Phys. Rev. **D52** (1995) 2656.

[28] E653 Collaboration, K.Kodama *et al.* Phys. Lett. **B316** (1993) 455.

[29] A.Bean *et al.*, Phys. Lett. **B317**, (1993) 647.

[30] F.J.Gilman *et al.* ref. [13] 94.

[31] P.Ball, V.M.Braun, hep–ph/9701238, and private communication

[32] B.Stech, Preprint HD–THEP–96–35.

[33] S.Sanghera *et al.*, Phys.Rev. **D47** (1993) 791.

[34] M.Neubert, *B Decays and CP Violation*, CERN-TH/96-55, to appear in International Journal of Modern Physics A.

[35] S.Narison Phys. Lett. **B283** (1992) 384.

[36] P. Ball, V.M. Braun, H.G. Dosch, Phys. Rev. **D44** (1991) 3567.

[37] UKQCD collaboration, D.R. Burford et al., Nucl. Phys. **B 447** (1995) 425.

[38] APE collaboration: C.R.Allton et al., Phys. Lett. **B345** (1995) 513.

[39] H-n. Li and H.-L. Yu, Phys. Rev. Lett. **74**, (1995) 4388.

[40] J.G. Körner and G.A. Schuler, Z. Phys. **C 38**, (1988) 511.

Figure Captions

Figures 1, 2, 3 and 4 The form factors $F_1(q^2)$ for $B \to D$, $B \to \pi$, $D \to K$ and $D \to \pi$ transitions, respectively, obtained using the ISGW parameters, but adopting the experimental values for the meson masses. The relation between the kinematical variables y and q^2 is given by Eq.(4). The solid lines are the results of our LF calculations obtained using Eq.(46) with $\alpha_1, \alpha_2 \to 0$. The dashed lines are the previous results of ref. [3] corresponding to the choice of the two reference frames with $\alpha_1 = 0$, $\alpha_2 = \pi$ as explained in the text. The corresponding decay rates are listed in Table 2.

Figures 5, 6, 7 and 8 The vector $V(q^2)$ and axial form factors $A_0(q^2)$, $A_1(q^2)$ and $A_2(q^2)$ for $B \to D^*$, $B \to \rho$, $D \to K^*$ and $D \to \rho$ transitions, respectively, obtained using the ISGW parameters, but adopting the experimental values for the meson masses. The solid, dashed, dotted and dot-dashed lines represent the vector form factor $V(q^2)$ and axial form factors $A_0(q^2)$, $A_1(q^2)$ and $A_2(q^2)$, respectively. The corresponding decay rates are listed in Table 2.

Figure 9 The $\frac{d\Gamma}{dq^2}$ distribution for $\bar{B} \to D^* \ell \nu_\ell$ decays. The upper thin line with $|V_{bc}| = 0.0374$ corresponds to our fit to the CLEO data [16] while the lower solid line corresponds to $|V_{bc}| = 0.036$ found from the partial width.

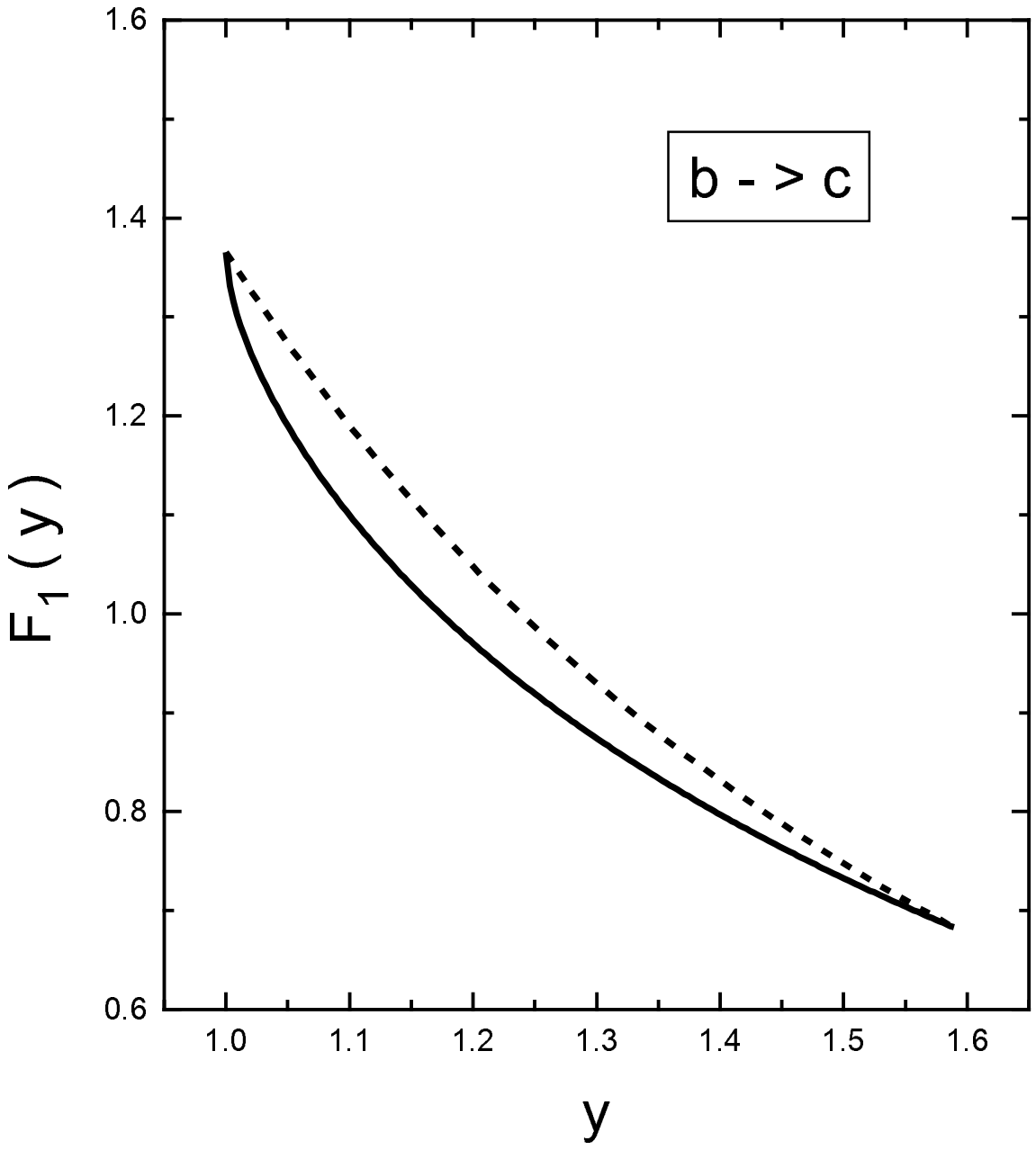

Figure 1: Form factor $F_1(q^2)$ for $B \to D$

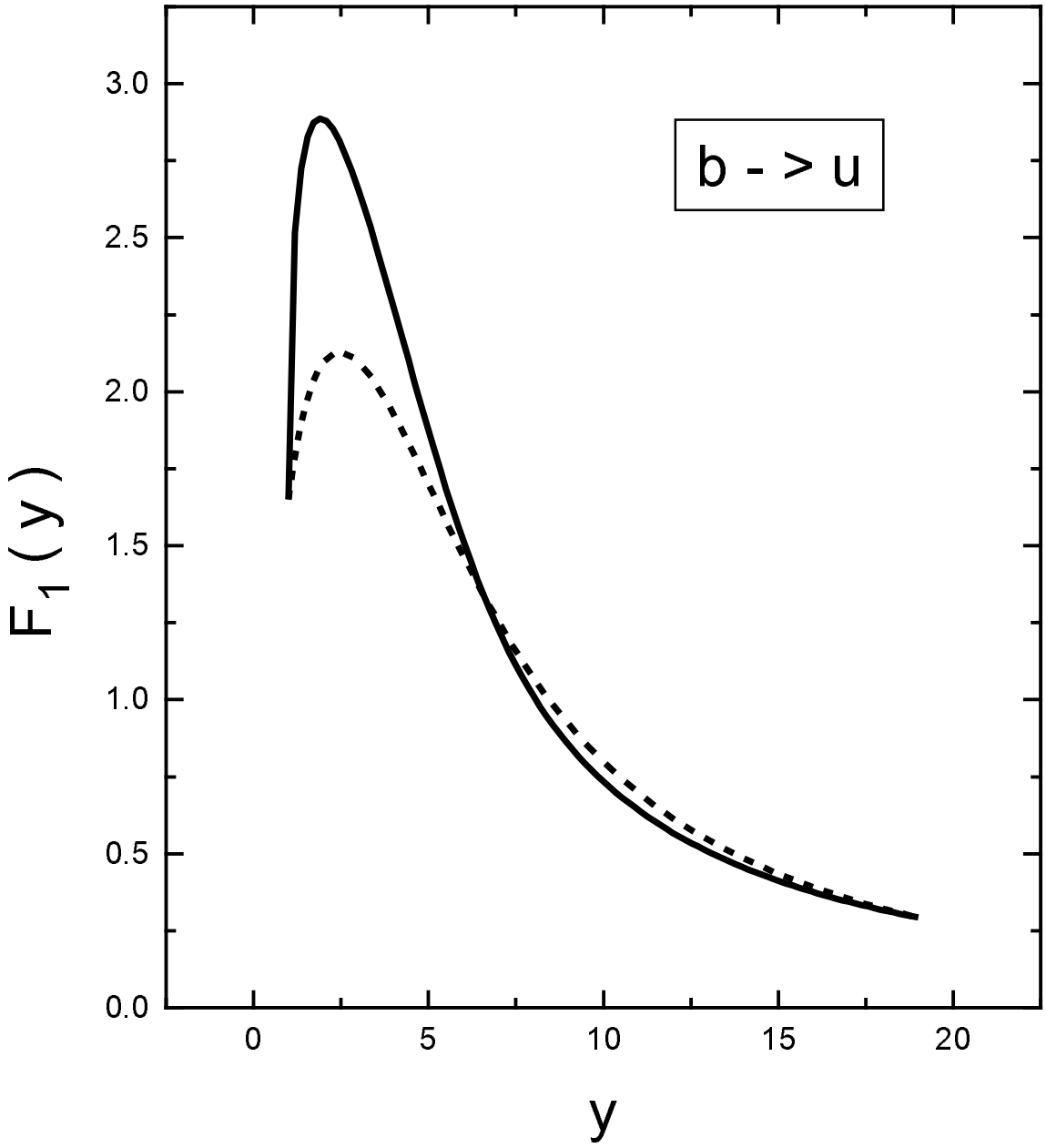

Figure 2: Form factor $F_1(q^2)$ for $B \to \pi$

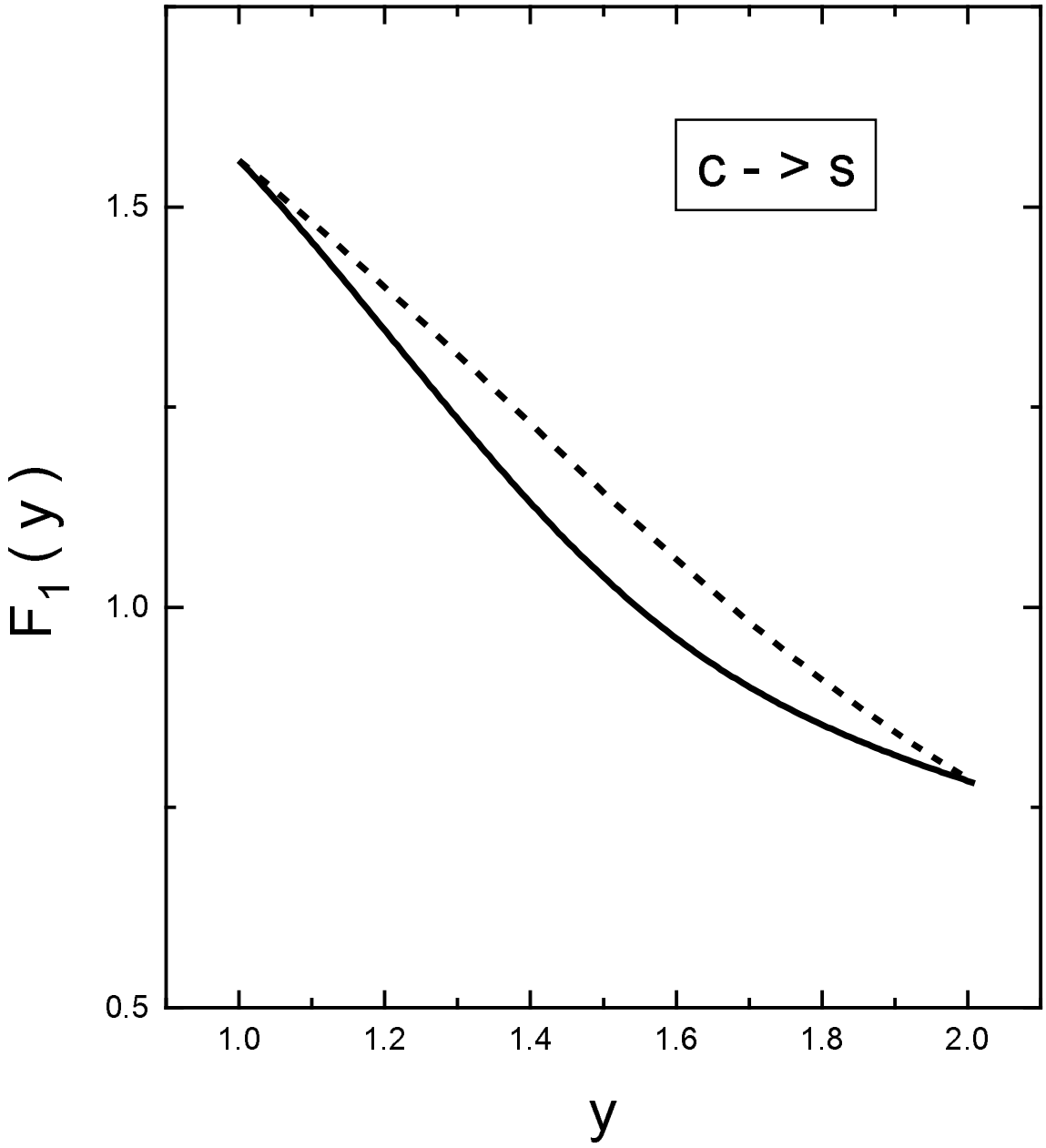

Figure 3: Form factor $F_1(q^2)$ for $D \to K$

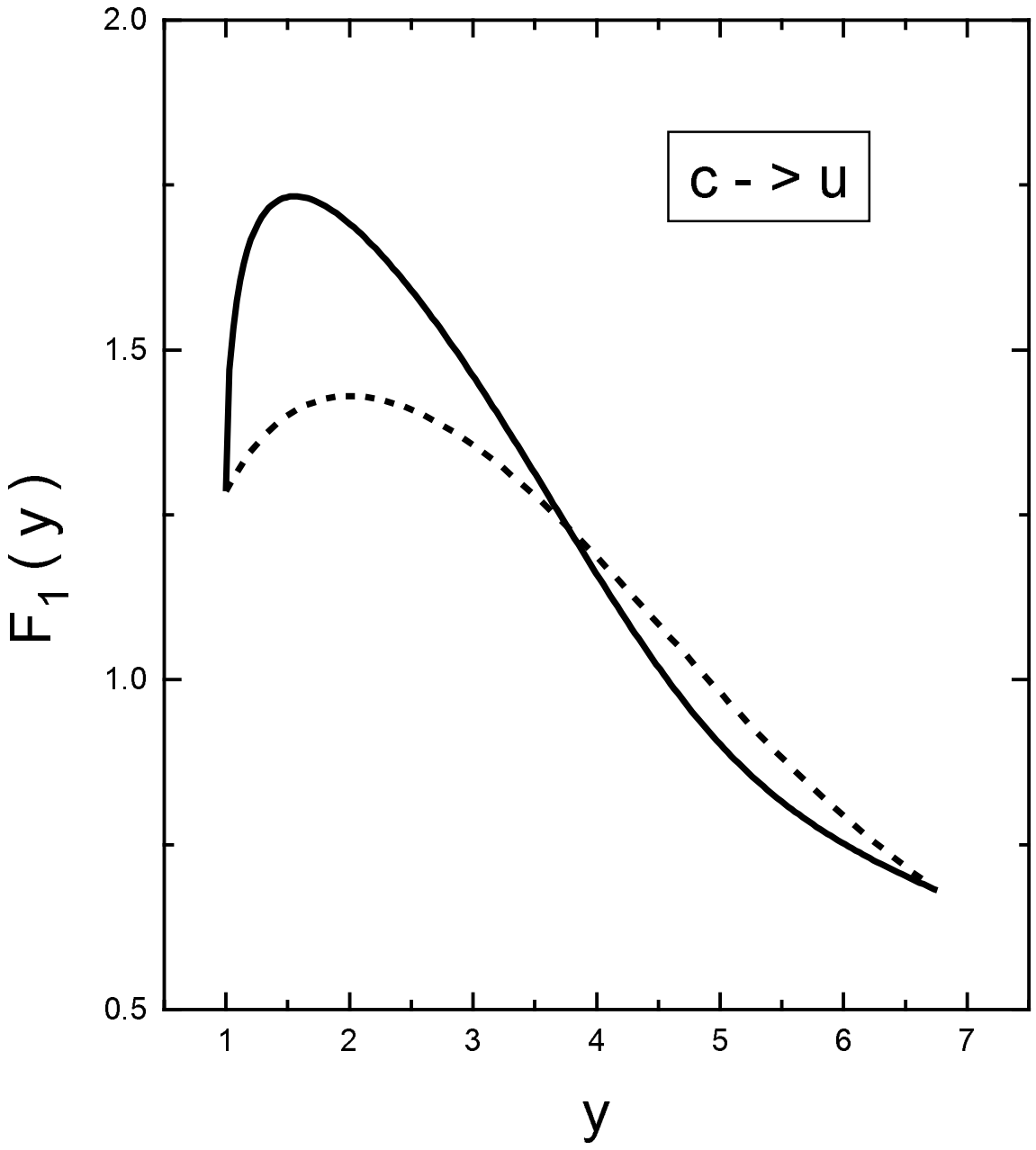

Figure 4: Form factor $F_1(q^2)$ for $D \to \pi$

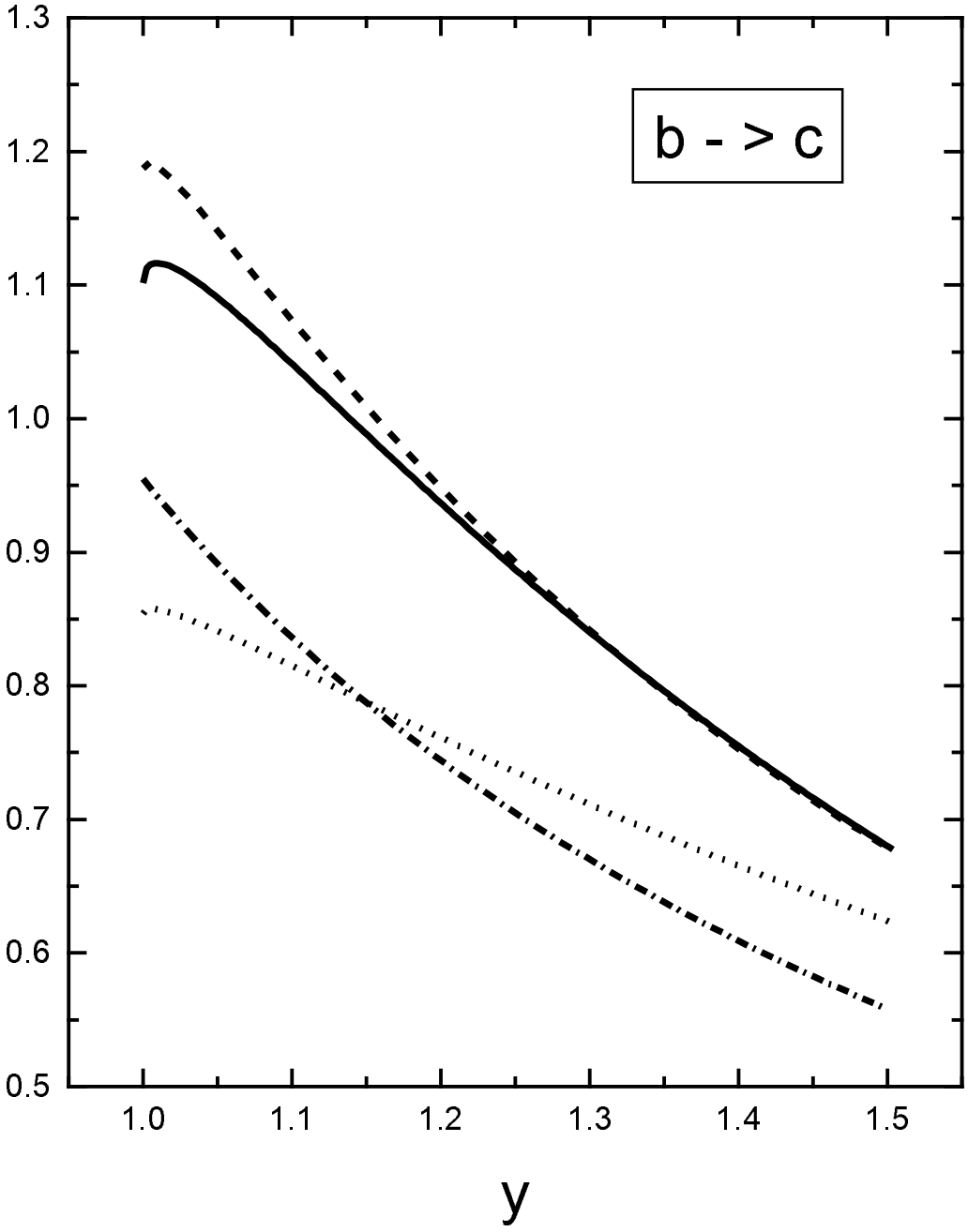

Figure 5: The vector $V(q^2)$ and axial form factors $A_0(q^2)$, $A_1(q^2)$ and $A_2(q^2)$ for $B \to D^*$.

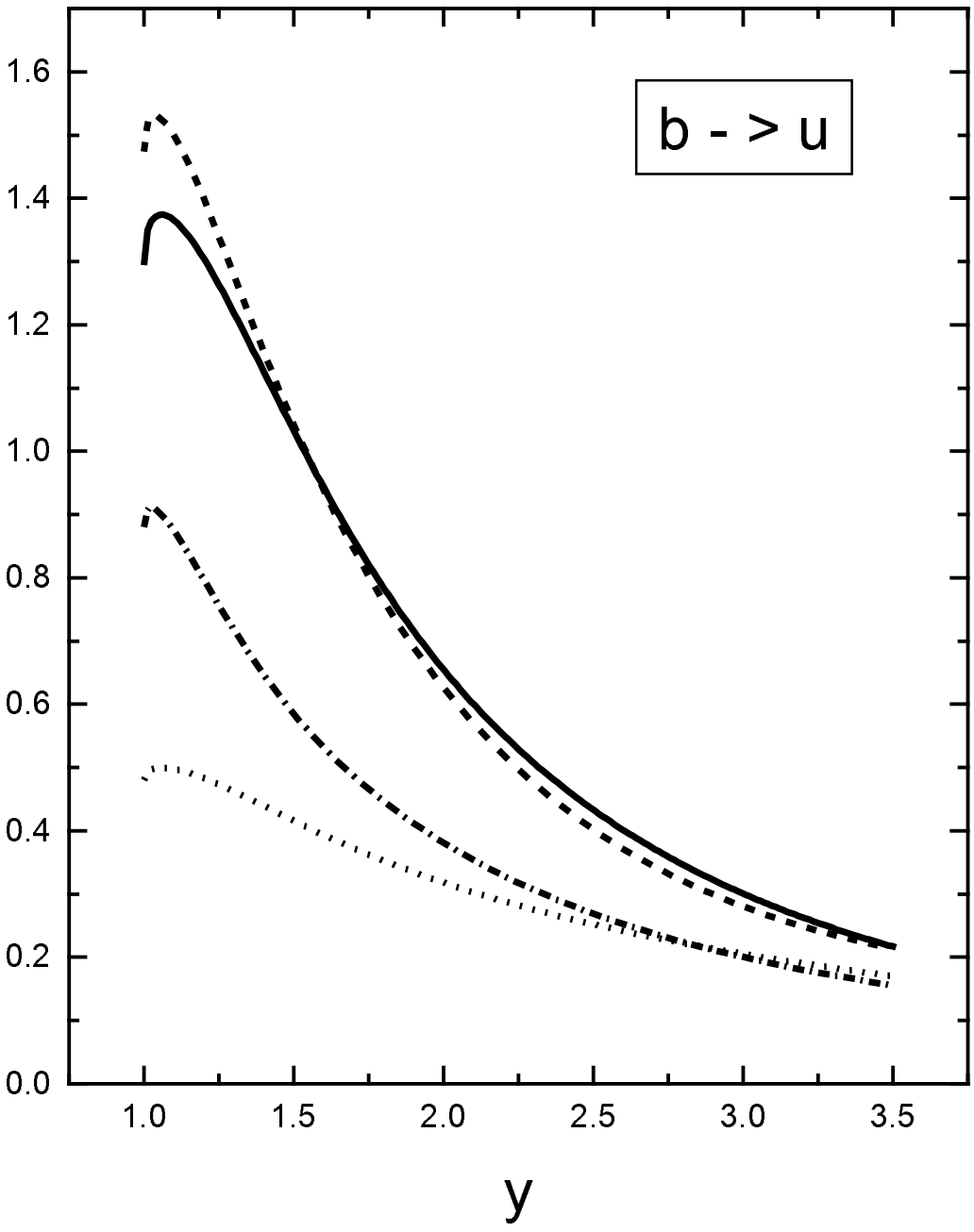

Figure 6: The vector $V(q^2)$ and axial form factors $A_0(q^2)$, $A_1(q^2)$ and $A_2(q^2)$ for $B \to \rho$.

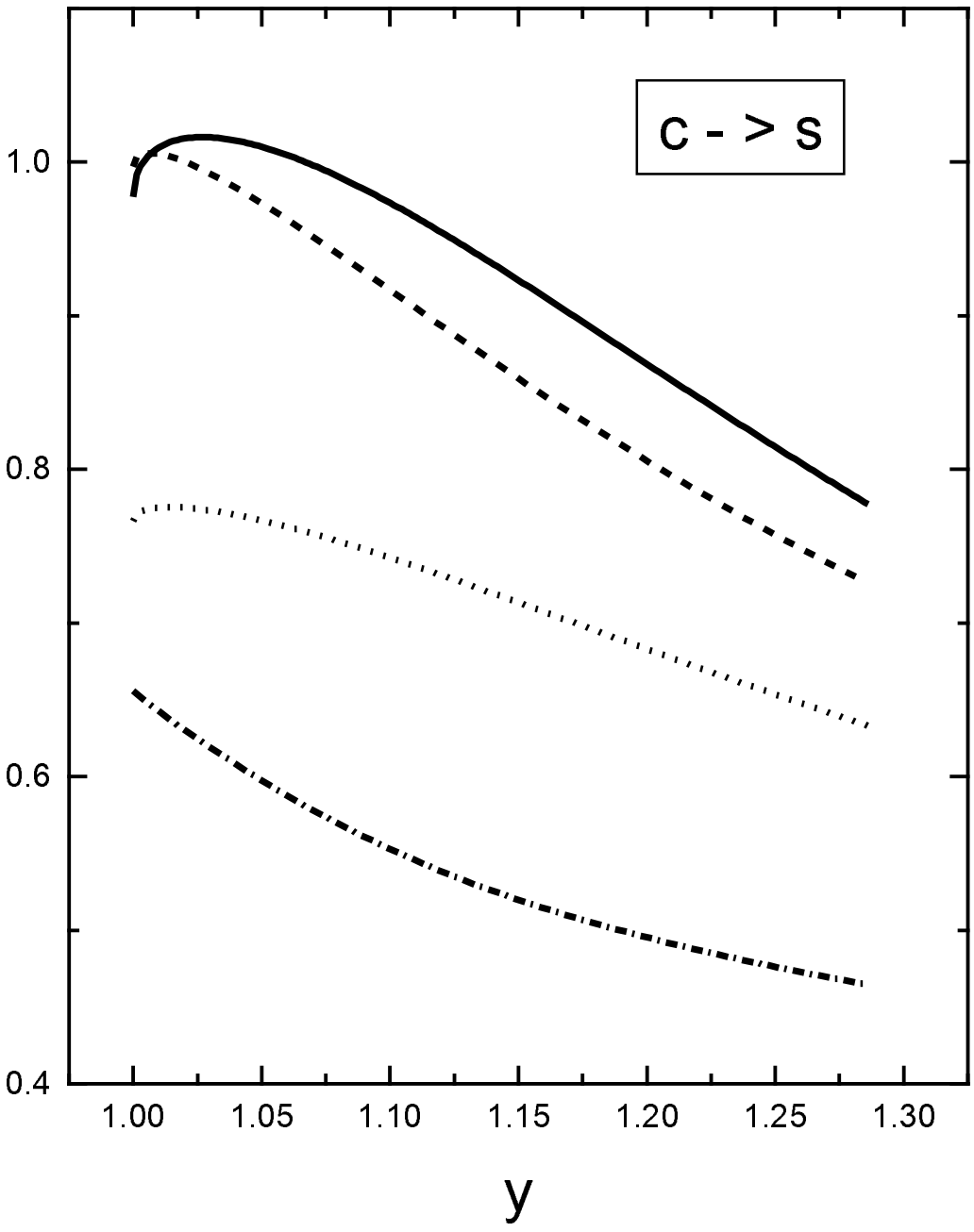

Figure 7: The vector $V(q^2)$ and axial form factors $A_0(q^2)$, $A_1(q^2)$ and $A_2(q^2)$ for $D \to K^*$.

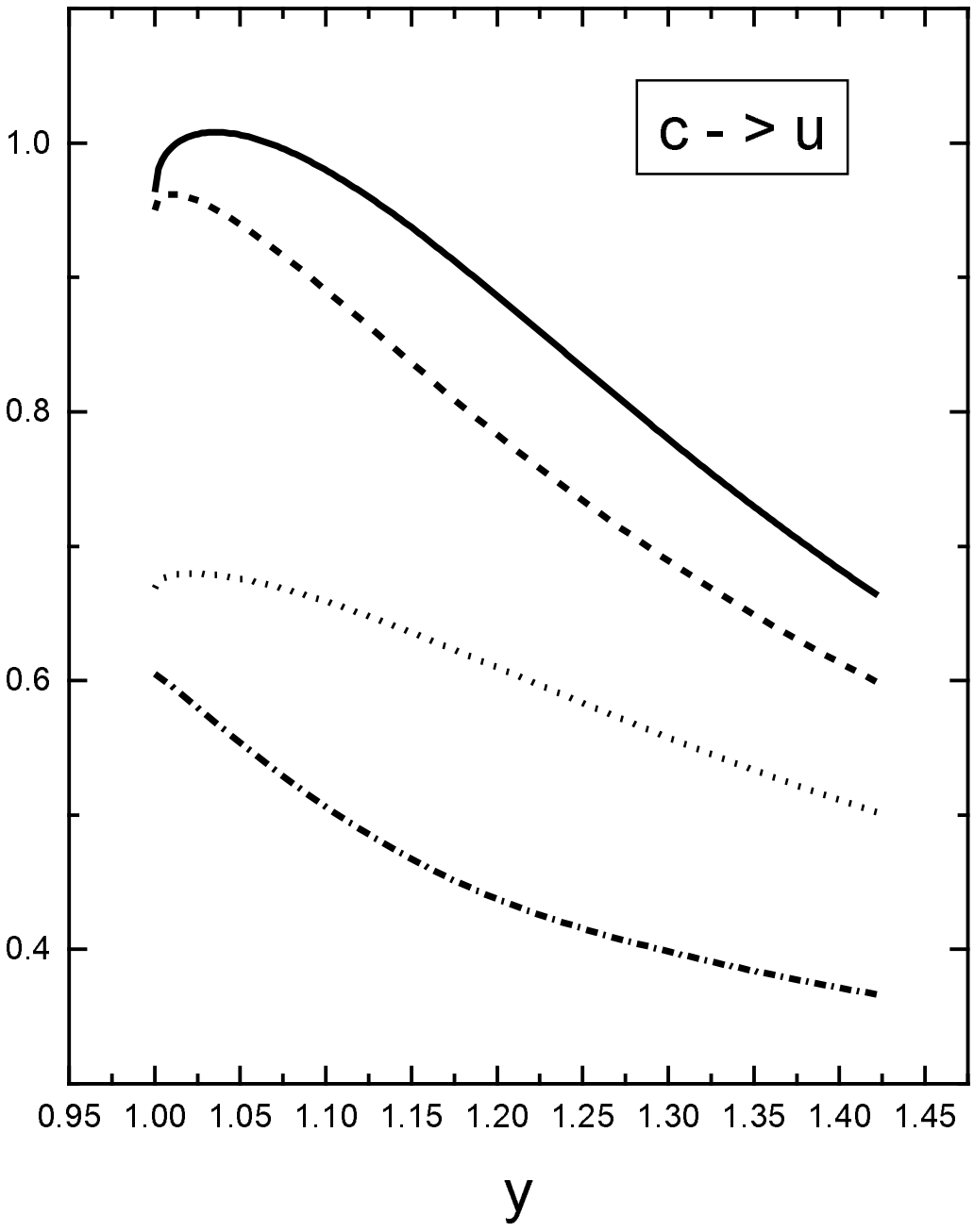

Figure 8: The vector $V(q^2)$ and axial form factors $A_0(q^2)$, $A_1(q^2)$ and $A_2(q^2)$ for $D \to \rho$.

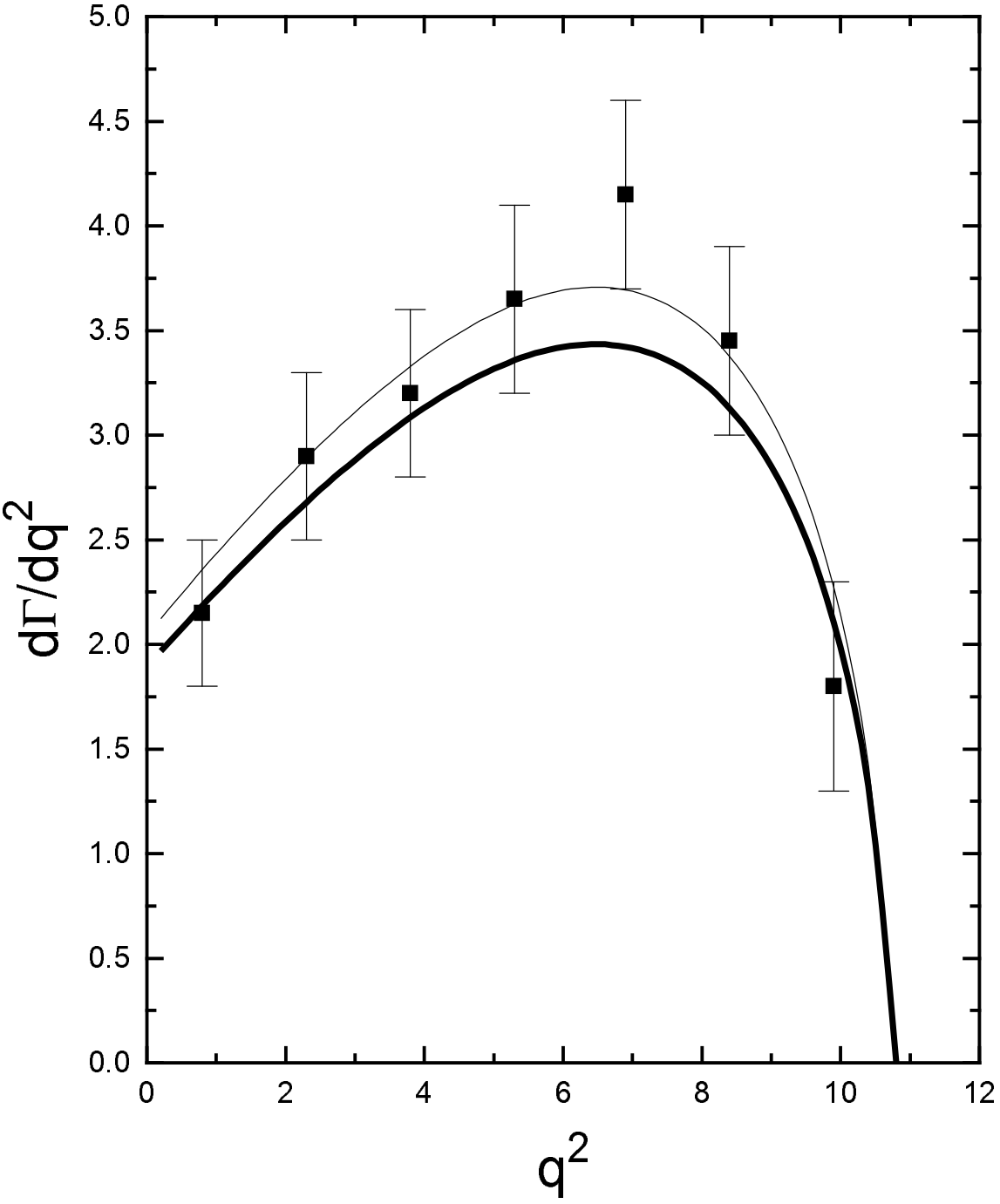

Figure 9: The $\frac{d\Gamma}{dq^2}$ distribution for $\bar{B} \to D^* \ell \nu_\ell$ decays.